SUPPORTING DATA INFORMATION

Fluorescent lipid nanoparticles as biomembrane models for exploring emerging contaminant bioavailability supported by density functional theory calculations

Miquel Oliver, Antonio Bauzá, Antonio Frontera* and Manuel Miró*

Department of Chemistry, University of the Balearic Islands, Carretera de Valldemossa km 7.5, 07122 Palma de Mallorca, Illes Balears, Spain

Corresponding authors:

Antonio Frontera. Department of Chemistry, University of the Balearic Islands, Carretera de Valldemossa km 7.5, 07122 Palma de Mallorca, Illes Balears, Spain.
E-mail: toni.frontera@uib.es. Tel: +34-971173498. FAX: +34-971173426.

Manuel Miró. FI-TRACE group, Department of Chemistry, University of the Balearic Islands, Carretera de Valldemossa km 7.5, 07122 Palma de Mallorca, Illes Balears, Spain.
E-mail: manuel.miro@uib.es. Tel: +34-971172746. FAX: +34-971173426.

Number of pages: 20

Number of schemes: 1

Number of figures: 6

Number of tables: 8

Relationship between Generalized fluorescence measurements and solvent polar relaxation

In non-polar membrane environments, the naphthalene fluorophore features a maximum-intensity wavelength in the fluorescence emission spectrum centred at 440 nm. However, a bathochromic Stokes (red) shift is observed upon increasing of membrane phase polarity, that is, membrane hydration, which is an indicator of the perturbation of the lipid nanoscale vesicles rendering a looser and disordered structure that might be measured semi-quantitatively by the decrease in GP values. This characteristic behaviour is a consequence of solvent molecules surrounding the probe's fluorophore moiety to form dipole states and to reorientate along the fluorophore's dipole moment upon its excitation. This phenomenon is known as solvent dipolar relaxation and results in a red-shifted emission towards 490 nm as a result of the formation of a charge transfer excited state, stabilized by the water dipole reorientation process [1,2]. The more acute is the water relaxation process occurring in the vicinity of the probe the more significant the membranotropic effects are. Prodan serves to signal interactions on the polar moieties of PC while Laurdan does at the hydrophilic-hydrophobic interface of the lipid bilayer. The latter is harnessed in this work as a marker of enhanced contaminant penetration across the liposomal bilayer and thus indicates *in-vitro* bioavailability with potential in-vivo absorption by the systemic circulation. It should be also noted that exogenic compounds might also participate in supramolecular interactions leading to improved lipid packing as identified by hypsochromic (blue) shift towards 440 nm, with the subsequent increase in Laurdan GP, for which the liposomal nanoparticle behaviour resembles the gel phase more closely and the solvent dipolar relaxation process is lessened to a large extent.

Flow cytometry measurements

Working solutions of 50 µmol/L PC liposomes in buffer (10 mmol/L HEPES, 0.1 mol/L NaCl, pH 7.4) with and without the addition of a given concentration of EC were analyzed by flow cytometry. To this end, the liposomal nanoparticles were mixed and incubated with 10 µg/mL biocide (one at a time) for 1 h in the dark and room temperature. In each measurement, a nominal number of 10,000 events were recorded. Two dynamic scattering parameters were determined in every individual sample: the forward laser light scattering (FS) and the side laser light scattering (SS). The former gives insight into the vesicle size distribution and the latter relates to inner vesicle composition and complexity. Semi-quantitative population data were obtained with WinMDI 2.9 software.

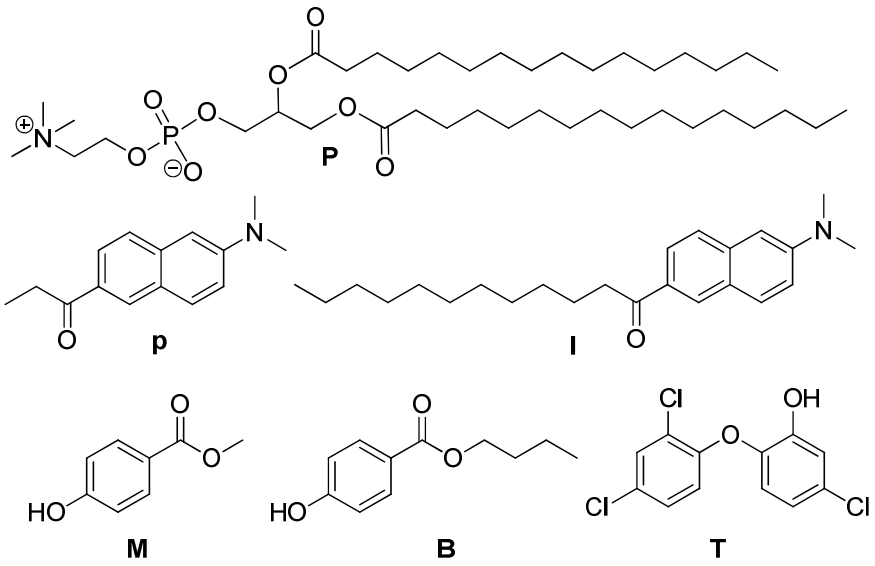

Scheme S1. Chemical structure of the phospholipid (16:0) PC model, fluorescent membrane probes and target contaminants explored in this work. **P**: Phosphatidylcholine. **p**: Prodan. **l**: Laurdan. **M**: Methylparaben. **B**: Butylparaben. **T**: Triclosan.

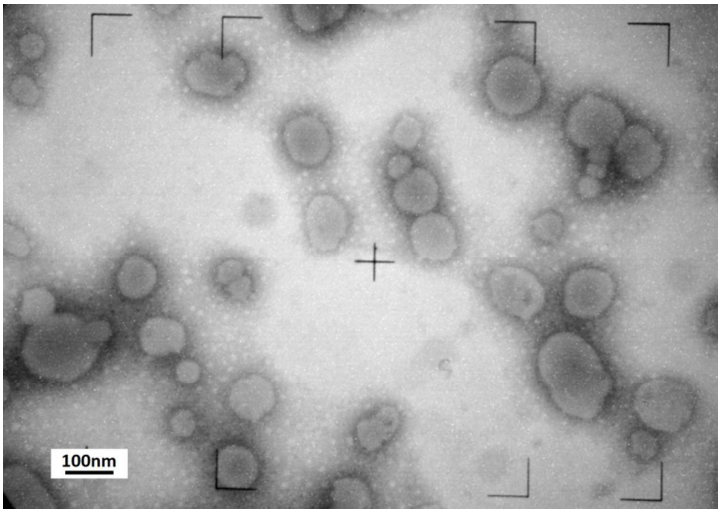

Figure S1. Transmission electron micrograph of soybean PC liposomes at the 4mg PC/mL level with a 80K magnification

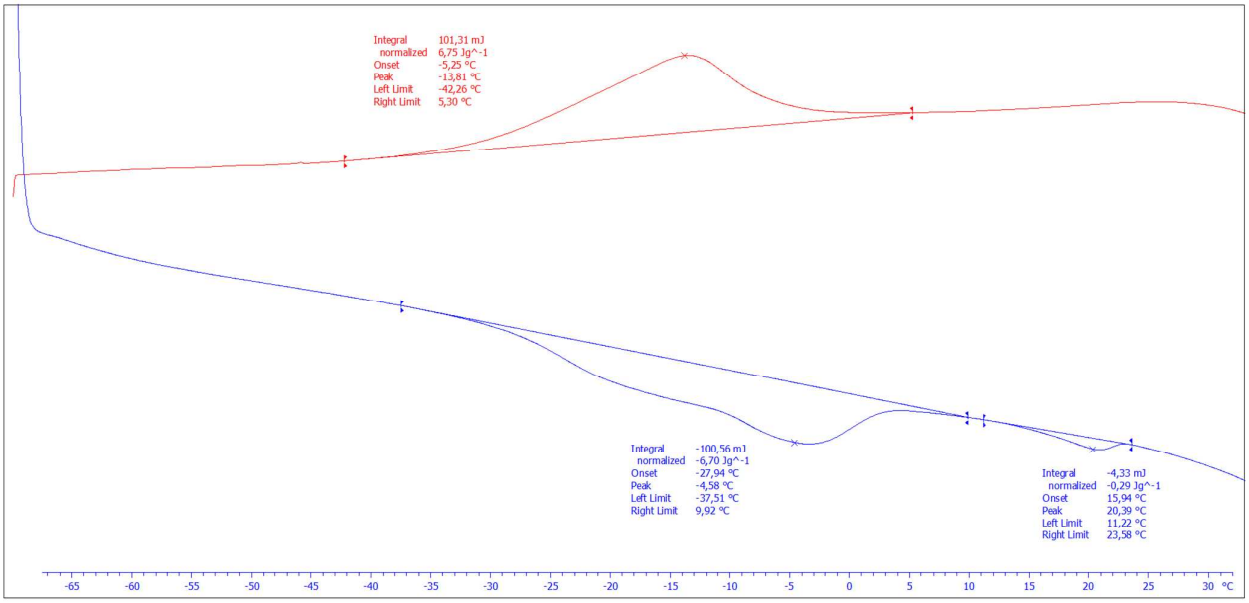

Figure S2. Differential scanning calorimetric (DSC) explorations of changes in soybean PC phase transition temperatures. DSC graph is obtained with a heating rate of 2.0 ºC/min within the -70 to 35 ºC range using 40µL aluminium sample vials.

Figure S3. 2D optical scattering plots for empty PC liposomes against PC liposomes in the presence of methylparaben (M), butylparaben (B) and triclosan (T)

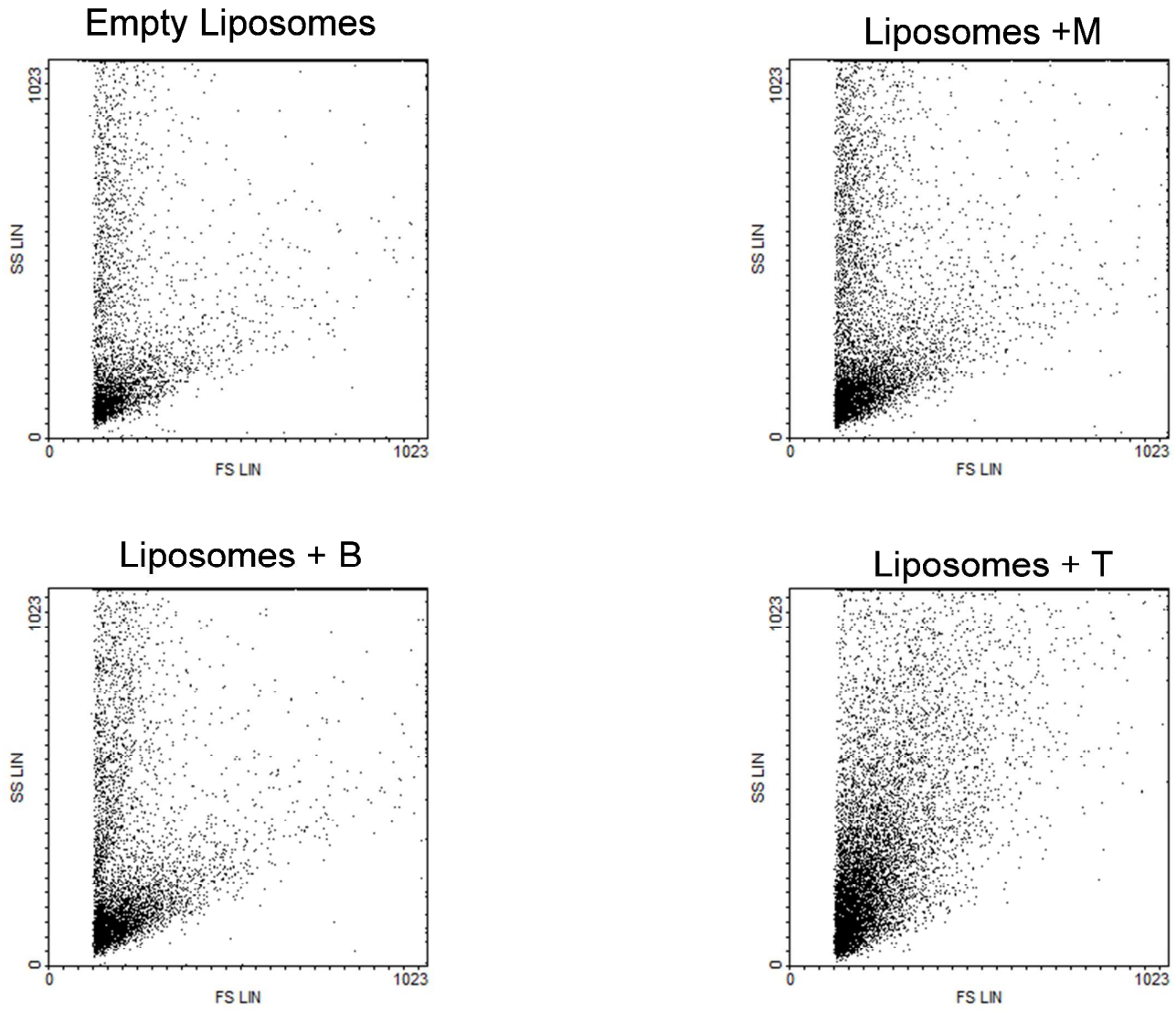

Figure S4. Side-scattered light profiles for empty PC liposomes against PC liposomes in the presence of methylparaben (M), butylparaben (B) and triclosan (T)

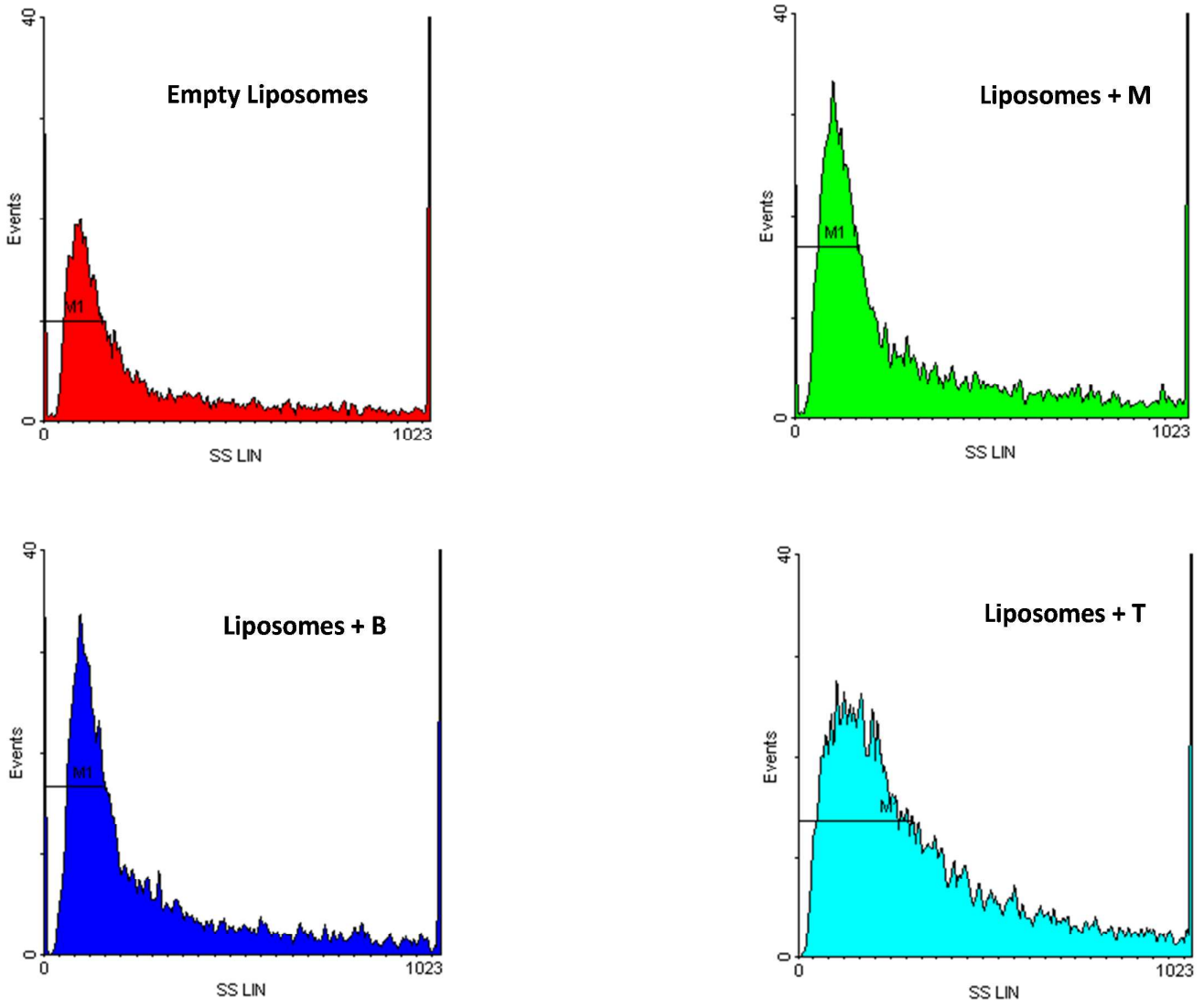

Figure S5. Steady-state fluorescence emission spectra of Laurdan-embedded PC liposomes with (T) and without (L) triclosan at 3 and 37ºC. Hypsochromic (blue) shifts and quenching effects of triclosan at the 10 μg/mL level are identified.

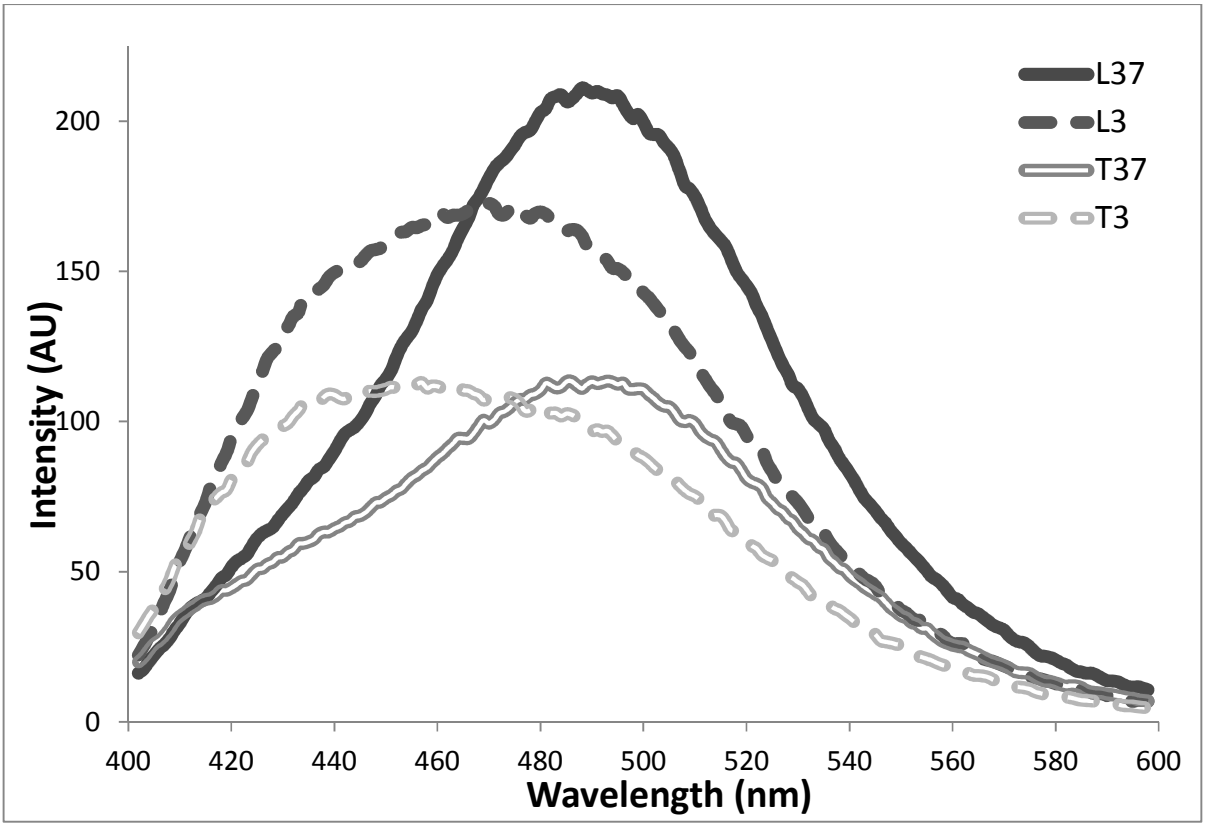

Figure S6. Prodan's GP fluorescence data of PC liposomes in the presence or absence of emerging contaminants in bioavailability testing. Experimental data are obtained at four different temperatures (3 ºC, 10ºC, 25ºC and 37ºC)

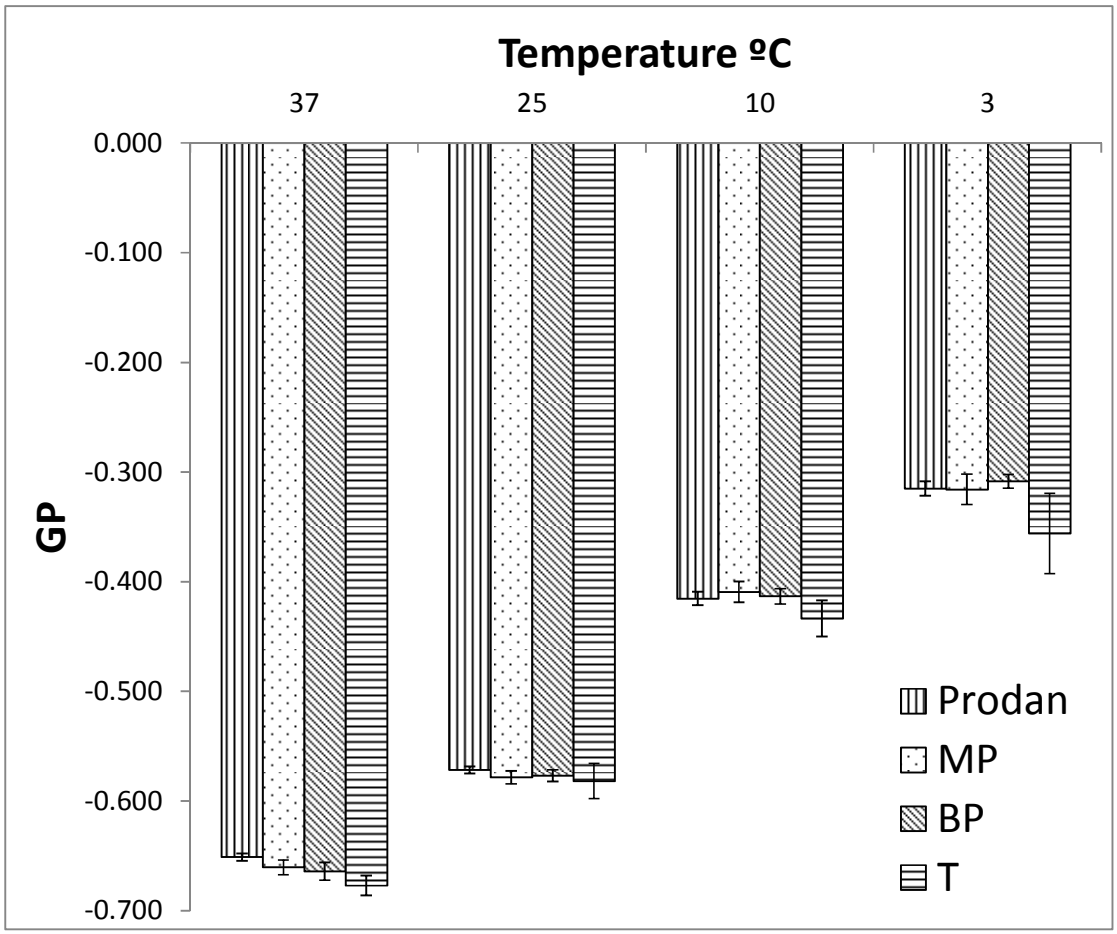

Table S1. Quantitative evaluation of EC permeability through PC liposomes by light scattering

Compound	MT	M1	M1/MT
Liposome	3,449	1,623	0.47
Methylparaben	5,856	2,815	0.48
Butylparaben	5,495	2,674	0.49
Triclosan	8,474	5,090	0.60

Table S2. Laurdan's GP fluorescence data for the investigated contaminants on the basis of the incubation temperature

	Laurdan	**Methylparaben**		**Butylparaben**		**Triclosan**	
Temperature (ºC)	**GP±SD**	**GP±SD**	t_{exp}	**GP±SDsd**	t_{exp}	**GP±SD**	t_{exp}
37	-0.481±0.003	-0.476±0.009	1.319[a]	-0.466±0.003	9.577[f]	-0.42±0.01	12.644[c]
25	-0.405±0.003	-0.40±0.02	1.271[b]	-0.378±0.004	15.520[f]	-0.33±0.01	20.388[d]
10	-0.249±0.004	-0.24±0.02	1.601[b]	-0.205±0.007	15.302[f]	-0.151±0.006	36.579[e]
3	-0.146±0.004	-0.13±0.03	1.329[b]	-0.095±0.008	15.982[f]	-0.045±0.006	38.407[e]

Note: The superscripts refer to the following critical *t*-values: a = 2.262, b= 2.365, c = 2.306, d = 2.571, e = 2.179 and f = 2.145

Table S3: Increase of Laurdan's GP fluorescence data for soybean PC liposomes in the presence of emerging contaminants in bioavailability testing at varied temperatures

	% GP Increase			
Temperature(ºC)	**37**	**25**	**10**	**3**
Methylparaben	0.9	1.8	4.9	9.5
Butylparaben	3.0	6.7	17.4	34.5
Triclosan	13.6	19.4	39.3	69.1

Experimental conditions. PC concentration: 50μM, Laurdan concentration: 2 μM, EC concentration: 10 μg/mL

Table S4. Prodan's GP fluorescence data for the investigated contaminants on the basis of the incubation temperature

	Prodan	Methylparaben		Butyparaben		Triclosan	
Temperature (ºC)	**GP±SD**	**GP±SD**	t_{exp}	**GP±SD**	t_{exp}	**GP±SD**	t_{exp}
37	-0.651±0.003	-0.660±0.007	2.491[a]	-0.664±0.008	2.545[a]	-0.677±0.009	5.438[b]
25	-0.572±0.003	-0.578±0.006	2.049[a]	-0.577±0.005	1.494[a]	-0.58±0.02	1.735[c]
10	-0.415±0.006	-0.409±0.009	1.061[a]	-0.413±0.007	0.376[a]	-0.43±0.02	2.087[b]
3	-0.315±0.007	-0.32±0.01	0.089[a]	-0.308±0.006	1.250[a]	-0.36±0.04	3.060[c]

Note: The superscripts refer to the following critical *t*-values: a = 2.447, b = 2.228 and c = 2.306

Table S5: Variation of Prodan's GP fluorescence data for soybean PC liposomes in the presence of emerging contaminants in bioavailability testing at varied temperatures

	% GP variation			
Temperature(ºC)	**37**	**25**	**10**	**3**
Methylparaben	-1.4	-1.2	1.4	-0.2
Butylparaben	-2.0	-0.9	0.5	2.1
Triclosan	-4.0	-1.8	-4.4	-13.0

Experimental conditions. PC concentration: 50μM, Prodan concentration: 2 μM, EC concentration: 10 μg/mL

Table S6. Fluorescence anisotropic measurements (r_{ss}) for the investigated contaminants on the basis of the incubation temperature

	Laurdan	**Methylparaben**		**Butylparaben**		**Triclosan**	
Temperature (ºC)	**r_{ss}±SD**	**r_{ss} ±SD**	**t_{exp}**	**r_{ss} ±SD**	**t_{exp}**	**r_{ss} ±SD**	**t_{exp}**
37	0.132±0.001	0.139±0.003	3.658[a]	0.135±0.002	1.191[a]	0.162±0.004	13.059[c]
25	0.1479±0.0008	0.152±0.002	4.184[a]	0.1498±0.0009	1.904[b]	0.170±0.003	14.945[a]
10	0.166±0.002	0.166±0.003	0.321[a]	0.167±0.001	1.059[a]	0.181±0.003	9.196[a]
3	0.1728±0.0007	0.172±0.002	0.581[a]	0.174±0.002	0.816[a]	0.187±0.004	7.511[c]

Note: The superscripts refer to the following critical *t*-values: a = 2.447, b = 2.571, c = 3.182

Table S7: Variation of fluorescence anisotropy data for soybean PC liposomes in the presence of emerging contaminants in bioavailability testing at varied temperatures

	% Variation of fluorescence anisotropy			
Temperature (ºC)	**37**	**25**	**10**	**3**
Methylparaben	4.7	2.8	0.3	-0.3
Butylparaben	2.2	1.3	1.0	0.9
Triclosan	22.3	15.1	9.5	8.4

Experimental conditions. PC concentration: 50μM, Laurdan concentration: 2 μM, EC concentration: 10 μg/mL

Table S8. Ecotoxicological and bioaccumulation data of target species

Target compound	*Vibrio fisheri* EC50 (15min)	*Daphnia magna* LC50 (48h)	*Pimephales promelas* LC50 (48h)	*Bioconcentration factor (*BCF*)* [3]
Triclosan	0.15-0.95 µg/mL [4-7]	0.39 µg/mL [8]	0.27 µg/mL [8]	368
Butylparaben	1.2-2.5 µg/mL [9,10]	5.3-9.2 µg/mL [8,10]	4.2 µg/mL [8]	112
Methylparaben	5.9-9.6 µg/mL [9,10]	24.6-62 µg/mL [8,10]	No effects found at concentrations exceeding water solubility (> 2.5 g/L) [8]	6.4

References

(1) Lakowicz J.R. (Ed.). *Principles of Fluorescence Spectroscopy, 3rd Edition*; Springer Science+Business Media: New York, 2006; chap. 6 and 7.

(2) Viard, M.; Gallay, J.; Vincent, M.; Meyer, O.; Robert, B.; Paternostre, M. Laurdan solvatochromism: solvent dielectric relaxation and intramolecular excited-state reaction. *Biophys. J.* **1997**, *73* (4), 2221–2234.

(3) United States Environmental Protection Agency, *Estimation Programs Interface Suite™ for Microsoft® Windows*, US EPA, Washington, DC, USA, 2015. Available at: http://www.epa.gov/tsca-screening-tools/epi-suitetm-estimation-program-interface

(4) Rosal, R.; Rodea-Palomares, I.; Boltes, K.; Fernández-Piñas, F.; Leganés, F.; Petre, A. Ecotoxicological assessment of surfactants in the aquatic environment: combined toxicity of docusate sodium with chlorinated pollutants. *Chemosphere* **2010,** *81*(2), 288-293.

(5) Farré, M.; Asperger, D.; Kantiani, L.; González, S.; Petrovic, M.; Barceló, D. Assessment of the acute toxicity of triclosan and methyl triclosan in wastewater based on the bioluminescence inhibition of Vibrio fischeri. *Anal. Bioanal .Chem.* **2008**, *390* (8), 1999–2007.

(6) Tatarazako, N.; Ishibashi, H.; Teshima, K.; Kishi, K.; Arizono, K. Effects of triclosan on various aquatic organisms. *Environ Sci.* **2004**, 11(2), 133-140.

(7) Lopez-Roldan, R.; Kazlauskaite, L.; Ribo, J.; Riva, M.C.; González, S.; Cortina, J.L. Evaluation of an automated luminescent bacteria assay for in situ aquatic toxicity determination. *Sci. Total Environ.* **2012**, *440*, 307-313.

(8) Brausch, J.M.; Rand, G.M. A review of personal care products in the aquatic environment: environmental concentrations and toxicity. *Chemosphere* **2011**, *82* (11), 1518- 1532.

(9) Bazin I, Gadal A, Touraud E, Roig B. Hydroxy benzoate preservatives (parabens) in the environment: data for environmental toxicity assessment. *In Xenobiotics in the Urban Water Cycle: Mass Flows, Environmental Process, Mitigation and Treatment Strategies*; Fatta-Kassinos, D.; Bester, K.; Kümmerer, K. (Eds); Environmental Pollution, Vol 16, Springer Science+Business Media B.V: Heidelberg, 2010, ch. 14, pp. 245-257.

(10) Terasaki, M.; Makino, M.; Tatarazako, N. Acute toxicity of parabens and their chlorinated by-products with Daphnia magna and Vibrio fischeri bioassays. *J. Appl. Toxicol*. **2009**, *29* (3), 242–247.